Global influence of the AD1600 eruption of Huaynaputina, Peru

Shanaka L. de Silva & Gregory A. Zielinski

Reprinted from Nature, Vol. 393, June 4, 1998 Issue

Global influence of the AD1600 eruption of Huaynaputina, Peru

Shanaka L. de Silva* & Gregory A. Zielinski†

* *Department of Geography, Geology, and Anthropology, Indiana State University, Terre Haute, Indiana 47809, USA*
† *Climate Change Research Center, University of New Hampshire, Durham, New Hampshire 03824-3525, USA*

It has long been estabished that gas and fine ash from large equatorial explosive eruptions can spread globally, and that the sulphuric acid that is consequently produced in the stratosphere can cause a small, but statistically significant, cooling of global temperatures[1,2]. Central to revealing the ancient volcano–climate connection have been studies linking single eruptions to features of climate-proxy records such as found in ice-core[3–5] and tree-ring[6–8] chronologies. Such records also suggest that the known inventory of eruptions is incomplete, and that the climatic significance of unreported or poorly understood eruptions remains to be revealed. The AD1600 eruption of Huaynaputina, in southern Peru, has been speculated to be one of the largest eruptions of the past 500 years; acidity spikes from Greenland and Antarctica ice[3–5], tree-ring chronologies[6–8], along with records of atmospheric perturbations in early seventeenth-century Europe and China[9,10], implicate an eruption of similar or greater magnitude than that of Krakatau in 1883. Here we use tephra deposits to estimate the volume of the AD1600 Huaynaputina eruption, revealing that it was indeed one of the largest eruptions in historic times. The chemical characteristics of the glass from juvenile tephra allow a firm cause–effect link to be established with glass from the Antarctic ice, and thus improve on estimates of the stratospheric loading of the eruption.

Volcan Huaynaputina, located at 16° 35′ S, 70° 52′ W in the Moquegua region of southern Peru (Fig. 1), consists of three craters situated at 4,500 m within the amphitheatre of an ancient strato-volcano. A compilation of historical and parochial literature[11] reveals that the volcano formed during an eruption that began on 19 February 1600 and continued until 5 March. The fall deposit covered an area of at least 300,000 km^2 in southern and west central Peru, western Bolivia and north Chile (Fig. 1). Ashfall was reported on the major cities of Lima, La Paz (Bolivia) and Arica (Chile) as well as on a ship 1,000 km to the west[11]. The fall seems to have been distributed predominantly to the west and north. Local proximal pyroclastic flows and secondary mass flows were insignificant in volume. This large plinian eruption destroyed local communities with a loss of over 1,000 lives and caused considerable damage to the major cities of Arequipa and Moquegua. The loss of farmland, crops, livestock, vineyards, and water resources compounded the significant economic burden on this region. The whole socio-economic infrastructure of a large part of Peru, and maybe that of

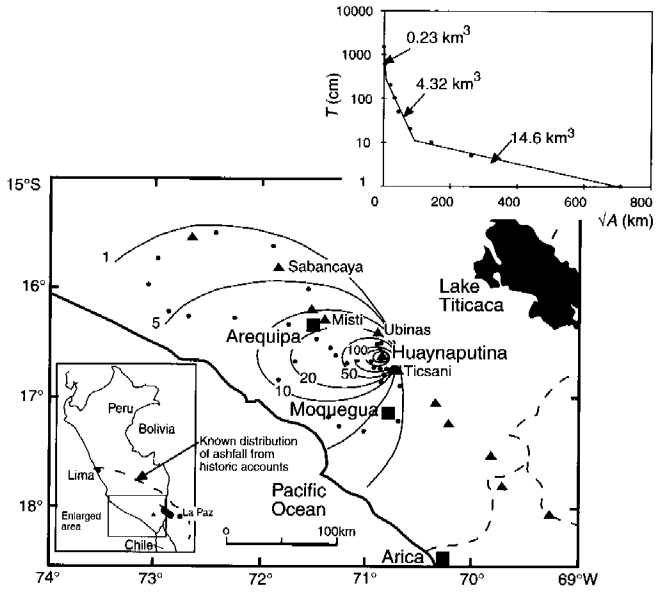

Figure 1 Isopach map of Huaynaputina tephra deposit showing the strong westerly distribution of the deposit. Black triangles are volcanoes of the modern volcanic arc and the most recently active are labelled; small dots are data points. Volcan Ticsani, the site of a similar but smaller eruption to Huaynaputina, is also shown. Values associated with contours are in centimetres; two innermost contours not labelled are 200 and 600 cm respectively, and the 1,500 cm contour is covered by the symbol for the volcano. The graph in the upper right corner shows a plot of thickness (T) on a logarithmic scale against the square root of isopach area[31,32]. The thickness data are described by three line segments that define a typical exponential profile. Integration beneath the line segments with respect to area, following the method of Fierstein and Nathenson[32], and removing the volume achieved by extrapolating the data to zero thickness[31], yields the volumes noted for each segment and the minimum volume of tephra of 19.2 km^3. Negative error in this estimate is limited to measurement and area estimation errors and is ~10% for this data set. Positive errors far outweigh this, as discussed in the text. Inset (bottom left) shows the known distribution of the fall from the AD1600 eruption (broken line) based on a compilation of parochial and historical accounts[11]. The box in the inset shows the area covered in the larger map. Note that our data cover only a small portion of the known distribution of the AD1600 tephra fall, albeit along the main axis. As most of the distal tephra has been lost, a considerable volume of distal tephra cannot be measured.

Table 1 Main oxide composition of individual juvenile clasts and volcanic glass from the Huaynaputina eruption compared with tephra from the early 1600s of the Antarctica and Greenland ice cores

	Huaynaputina bulk rock* (21 samples)	Huaynaputina glass* (n = 103; 6 samples)	Huaynaputina glasst (n = 7)	South Pole glasst (n = 16)	GISP2 glass* (n = 16)
SiO_2	65.16 ± 0.70	72.82 ± 0.68	75.76 ± 0.53	72.92 ± 2.04	62.1 ± 4.7
TiO_2	0.58 ± 0.03	0.26 ± 0.20	0.27 ± 0.06	0.34 ± 0.20	1.1 ± 0.5
Al_2O_3	16.68 ± 0.40	15.20 ± 1.21	13.85 ± 0.15	13.98 ± 0.91	16.2 ± 2.5
FeO	3.97 ± 0.17	1.31 ± 0.25	1.10 ± 0.14	1.37 ± 0.28	8.2 ± 3.5
MgO	1.78 ± 0.12	0.30 ± 0.13	0.27 ± 0.14	0.44 ± 0.20	1.9 ± 1.0
CaO	3.88 ± 0.17	1.61 ± 0.32	1.22 ± 0.07	1.41 ± 0.35	3.9 ± 1.7
Na_2O	4.57 ± 0.09	4.53 ± 0.34	3.43 ± 0.24	4.12 ± 0.73	4.0 ± 1.1
K_2O	2.79 ± 0.15	3.82 ± 0.18	3.89 ± 0.15	3.76 ± 0.28	2.5 ± 0.9

Errors are 1σ. n = number of individual analyses. Bulk rock analyses are of juvenile clasts from proximal and medial locations.
* This study.
† From ref. 16.

Table 2 Climate proxy data and atmospheric phenomena indicative of explosive volcanism in the earliest 1600s with known eruptions AD 1600–04

Ice core data

Location	Signal type/characteristics	Year of signal with error	Total volcanic flux kg km^{-2} (time)	Stratospheric mass loading (Mt)	
				Huaynaputina	Tambora
Greenland					
GISP2[4]	SO_4^{2-} doublet	1603–04 (±2)	36 (2 yr)	87	86
GRIP[21]	ECM doublet	1601–02 (±1)	36 (2.3 yr)	52	38
	SO_4^{2-} doublet	1601–02 (±1)	54 (2 yr)	78	101
Crete[3]	ECM doublet	1601–02 (±1)	61 (2 yr)	50	150
Antarctica					
South Pole[5]	SO_4^{2-} peak	1601 (±5)	22.5 (3–4 yr)	100	307
Siple Station[22]	SO_4^{2-} peak	1599 (±2)	34 (~4 yr)	n.d.	n.d.
Dyer Plateau[22]	SO_4^{2-} peak	1599 (±2)	30 (~4 yr)	n.d.	n.d.

Tree ring

Phenomenon	Location	Year	Comment
Narrow ring widths	Fennoscandia	1601	Calibrated to fourth coldest summer over past 1,500 years[23]
	Western USA	1601	Calibrated to coldest summer in most of western North America over past 400 years[24]
	Northern Hemisphere	1601	Calibrated to coldest summer over past 600 years[7,8]
	Sierra Nevada	1601	Cold summer[25]
Frost rings	Western USA	1601	Below freezing temperatures during growing season[6]
Light rings	Upper tree line, Quebec	1601 and 1603	Cold temperatures near end of growing season[26]

Atmospheric phenomena

Location	Comments
Scandinavia	Sun dimmed by constant haze in 1601 (ref. 9)
Central Europe	All through 1601 until the end of July 1602. Sun and Moon "reddish, faint and lacked brilliance". These phenomena led to minimum total (1601–04) dust veil index (DVI) estimate of 1,000 by comparison with phenomena associated with 1883 Krakatau and 1783 Laki eruptions (ref. 9).
Iceland	Summer of 1601, Sun pale and sunlight so faint that shadows not cast. Sky appeared cloudy and pale even when no clouds present. Winter of 1601–02 extremely severe (G. Larsen, personal communication, after ref. 27).
China	1603, red and dim Suns; 1604, large sunspots (ref. 10).
Graz, Austria	Darkened partial lunar eclipse in December 1601 implies a Northern Hemisphere average optical depth of 0.10, comparable to El Chichón and Agung, although if the dimness of the December 1601 partial eclipse was from Huaynaputina aerosols, then the 0.10 optical depth would not have been the maximum optical depth, but an optical depth following almost two years of aerosol loss from the stratosphere (R. Keen, personal communication after refs 28, 29).

Potential source eruptions (ref. 30 unless stated otherwise)

Volcano (latitude) tephra	Date of eruption	VEI	Volume (km^3)
Asama (Japan, 36° N)	January 1600	3?	?
Huaynaputina (Peru, 17° S) (this work)	February 1600	6	>19
Suwanose-Jima (Ryuku Is., 30° N)	1600 (year questionable)	4+	?
Iwaki (Japan, 41° N)	February 1604	3?	?

n.d., not determined, but considering that flux values are slightly higher than the South Pole values, loading estimates would be similar to or slightly above the 100 Mt estimate.

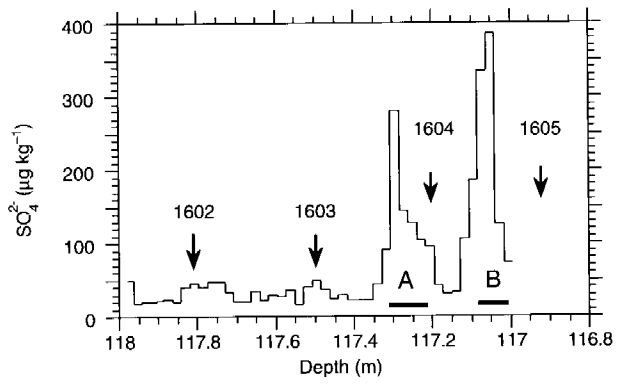

◀ **Figure 2** Subseasonal record of sulphate concentrations in the GISP2 ice core for the period AD1601–05. Arrows denote mid-summer for the year shown. Maximum dating error for this period is only ~2 years. It is believed, from correlation with the other ice cores, that the ages shown might be 1 or 2 years too young, although the red Suns observed in China in 1603 (Table 2) indicate that there still was a significant stratospheric aerosol loading in that year. Deposition of those aerosols on Greenland could easily have been in 1604. Even if the two sulphate spikes correspond to 1601/1602 and 1602/1603, these are ages within the error of the GSIP2 dating shown on the figure. Flux of the volcanic sulphate component of the record is 13 kg km^{-2} per 0.5 year for peak A and 21 kg km^{-2} per 0.5 yr for peak B from the detailed (~14 samples yr^{-1}) results presented here. Total volcanic flux of 34 kg km^{-2} per 2 yr agrees well with the 36 kg km^{-2} per 2 yr obtained from the original biyearly sampling done on the GISP2 core[4] and given in Table 1. Total volcanic sulphate flux is determined by the sum of the products of concentration, measured ice density and length for each sample. Volcanic sulphate concentration is the total concentration minus average background levels. Sea-salt sulphate was removed from the calculations. A and B also indicate the length of sections of ice filtered in an attempt to locate and identify volcanic glass with a scanning electron microscope and electron microprobe. Figure modified from ref. 4.